Self-Seeded Growth of Germanium Nanowires: Coalescence and Ostwald Ripening

*Olan Lotty[†,ϕ], Richard Hobbs[†,ϕ], Johann Hlina[§], Christoph Marschner[§], Colm O'Dwyer[†], Nikolay Petkov[†,ϕ] and *Justin D. Holmes[†,ϕ]*

[†]Materials Chemistry and Analysis Group and Applied Nanoscience Group, Department of Chemistry, University College Cork, Ireland and the Tyndall National Institute, University College Cork, Cork, Ireland. [ϕ]Centre for Research on Adaptive Nanostructures and Nanodevices (CRANN), Trinity College Dublin, Dublin 2, Ireland. [§]Institut für Anorganische Chemie der Technischen Universität Graz, Stremayrgasse 16, A-8010 Graz, Austria.

KEYWORDS: Germanium, Nanowires, Self-Seeded, Coalescence, Ostwald Ripening

Abstract

We report the controlled self-seeded growth of highly crystalline Ge nanowires, in the absence of conventional metal seed catalysts, using a variety of oligosilylgermane precursors and mixtures of germane and silane compounds (Ge:Si ratios between 1:4 and 1:1). The nanowires produced were encased in an amorphous shell of material derived from the precursors, which acted to isolate the Ge seed particles from which the nanowires were nucleated. The mode diameter and size distribution of the nanowires were found to increase as the growth temperature and Ge content in the precursors increased. Specifically, a model was developed to describe the main stages of self-seeded Ge nanowire growth (nucleation, coalescence and Ostwald ripening) from the oligosilylgermane precursors and in conjunction with TEM analysis, a mechanism of growth was proposed.

Introduction

Germanium nanowires have attracted considerable interest as a channel material for field-effect transistors (FETs) due to their lower resistivity and high hole carrier mobility, compared to silicon nanowires.[1] Recently, Ge nanowires have also been utilized for lithium battery anode materials, due to their higher rate of lithiation compared to silicon nanowires.[2] Furthermore, studies have shown that coating Ge nanowires with amorphous materials increases the reversible charge capacity of batteries made with Ge nanowire electrodes.[3] The synthesis of Ge whiskers, via a vapour-liquid-solid (VLS) growth mechanism, was first reported by Bootsma *et al.*[4] in 1971 and the synthesis of Ge nanowires, using a solvothermal approach, was subsequently reported by Heath and co-workers in 1993.[5] Many methods have since been developed for generating Ge nanowires, which can be found in a number of comprehensive review articles.[6] The Ge nanowire synthesis method progressed in this study is the lesser- reported self-seeded (or seedless) supercritical fluid (SCF) phase approach.[7] This self-seeded method does not rely on the growth of nanowires by a (noble) metal catalyst, but solely relies upon the

decomposition of metalorganic precursors to form a one dimensional (1D) structure. Whilst excellent levels of aspect control and scalability of semiconductor nanowires have been demonstrated using metal seeds, these catalysts can often contaminate, or uncontrollably dope, the growing nanowires.[8] For example, Korgel *et al.*[9], reported that at a eutectic temperature of 363 °C Ge atoms dissolve in Au nanocrystals to form a liquid AuGe eutectic alloy. This eutectic, while crucial to the growth of the nanowires via a supercritical-fluid-liquid-solid mechanism, can also provide a pathway for the diffusion of metal atoms from the seed into the semiconductor nanowire material. Solid phase seeding mechanisms for growing Ge nanowires, such as reported those using Ni catalyst seeds, were at first thought to limit this diffusion, but recent electrical results indicate that inadvertent doping still occurs.[10]

Here we report the growth Ge nanowires in the absence of conventional metal seeds using various mixtures of Ge and Si-containing precursors. Analysis of the diameter distributions of the nanowires grown in each of these experiments revealed several trends in growth behaviour, which can be directly linked to the precursor used and the temperature employed. We further propose that by analysing the statistical diameter distributions of the nanowires formed, in addition to extensive morphological characterisation by electron microscopy, the mechanism of nanowire growth can be inferred.

The coarsening of nanoparticles into nanowires via the self-seeded approach described in this article can occur through two fundamentally different mechanisms: (i) nanoparticles can move over a substrate, or within a matrix, to take part in binary collisions accompanied by liquid-like coalescence of the particles and (ii) the growth of nanowires can occur by the inter-particle transport of single atoms from smaller nanoparticles to larger nanoparticles known as Ostwald ripening.[11] Nanowire growth (length) and broadening (diameter) originates from the supersaturated phase, which is still present in the system after the nucleation stage and from concentration gradients around nanowires of different sizes.[12] The three main stages of nanowire growth (nucleation, coalescence and Ostwald ripening) are not sharply distinct, but in fact overlap during the evolution from a supersaturated phase to a ripened nanowire in the condensed phase.[13] We have combined a log-normal model for coalescence with a Gaussian model for

Ostwald ripening to create a equation that accounts for this overlap. The nanowires reported in this article were made with a variety of metalorganic precursors which were deliberately tuned to alter the Ge:Si ratio; the ratios investigated were 1:4, 1:3, 1:2 and 1:1. The Ge nanowires produced had a very uniform core diameter and were coated with a non-uniform shell consisting of Si, Ge, O and C. This amorphous coating was a by-product of the precursor decomposition and plays an important role in the nanowire growth process.

Experimental

The oligosilylgermane precursors 1,2-bis[tris(trimethylsilyl)germyl]tetramethyldisilane (Ge:Si 1:4), hexakis(trimethylsilyl)digermane (Ge:Si 1:3) and bis[tris(trimethylsilyl)germyl] dimethylgermane (Ge:Si 1:2) were synthesised following the procedures previously reported by Marschner *et al.*[14] For a 1:1 reaction mixture of Ge:Si, equal amounts of diphenylsilane (5 mM) and diphenylgermane (5 mM) were mixed together. The self-seeded growth of Ge nanowires was performed in a supercritical toluene medium using a method previously reported.[7] In a typical experiment, a 5 ml stainless steel reaction cell (HIP, USA) was loaded with 1 ml of anhydrous toluene and sealed inside a nitrogen filled glovebox. The reaction cell was then transferred to a tube furnace where it was heated to the desired reaction temperature and allowed to equilibrate for a period of 2 h. A Ge:Si precursor solution (10 mM), with a Ge:Si ratio of 1:4, 1:3, 1:2 or 1:1, was prepared in anhydrous toluene (10 ml) in a N_2 glovebox and loaded into a 20 ml stainless steel precursor reservoir (HIP, USA). This reservoir was then removed from the glovebox and connected to the reaction cell by 1/16" stainless steel tubing and valves. A back pressure of 17.2 MPa was applied to the precursor reservoir; this solution was injected at the chosen synthesis temperature using a CO_2 pump (ISCO systems). The volume of the precursor solution injected into the cell was dependent on the pressure difference between the reaction cell and that of the precursor reservoir. Typically, 2.5 ml of precursor solution was injected into the reaction cell, and the holding time adjusted according to the temperature employed for a high yield of Ge nanowires.[7] The cell was opened at room temperature, and the initial solvent was collected and

combined with an acetone solution used to collect the nanowire material attached to the side walls of the reactor. Energy dispersive X-ray (EDX) analysis was performed using an Oxford Instruments INCA system fitted to a TEM. High resolution transmission electron microscopy (TEM) images were collected using a JEOL 2100 HRTEM instrument operating at an acceleration voltage of 200 kV. In all cases, samples were prepared for analysis by sonicating the material in acetone before TEM sample preparation. Statistical analysis and modeling of the measured core diameter distributions of the nanowires was performed using Origin Pro v.8.5.1. and over 100 measurements were used for every nanowire diameter distribution (supporting information figures S3, S4 and S5).

Modelling Nanowire Growth

Links between the shape of diameter distributions of nanoparticles, nanoclusters and micro particles and their methods of growth (coalescence or Ostwald ripening) were established as early as 1976.[11] Accordingly, a log-normal shape seen in the size distribution curve of nanoparticles implies that the primary mechanism for growth can be inferred as coalescence. In this article, we extend this relationship from nanoparticles, nanoclusters and microparticles to nanowires. Ostwald ripening is often modelled with a function based upon the works of Lifshitz, Slyozof and Wagner.[15] Their combined methods have resulted in a model (LSW model) which is recognisable by its skewed distribution with a tail on the small diameter side of the diameter distributions. The LSW model also predicts that no particle greater than 1.5 times that of the mean particle diameter (in our case mean nanowire diameter) can exist. In reality, the particle size distributions are often skewed with a tail towards larger diameter sizes and particles greater than 1.5 times the average particle size often exist. The reason this upper limit exists is because LSW theory assumes that the system is infinitely dilute, which implies the absence of interparticle interactions.[16] Accounting for the stochastic process of interparticle interaction to and from particles, alters the LSW model and removes the artificial requirement that the particle size distribution, and all its derivatives, should go to zero above some finite value of particle size.[12] To address these experimentally observed shortfalls with the LSW model, many

groups have used a basic Gaussian function to model Ostwald ripening behaviour and have reported much better fits to experimentally obtained particle size distributions.[12, 17] A similar Gaussian function was incorporated into a model used by Conti *et al.*[18] who combined both coalescence and Ostwald ripening in a single model. Consequently, basic Gaussian and log normal functions were combined to account for the coalescence of Ge particles into nanowires in this study, as shown in equation 1. Formation of the combined log normal and Gaussian function in equation 1 is shown in supporting information figure S2, along with deconvoluted data highlighting the individual contribution of both functions.

$$y = y_0 + \frac{A_c}{\sqrt{2\pi}} \exp\left(\frac{-\ln\left(\frac{x}{x_c}\right)^2}{2\sigma^2} \right) + \frac{A_r}{\sigma_l \sqrt{\frac{\pi}{2}}} \exp\left(\frac{-2\left(x - x_{cg}\right)^2}{w_1^2} \right) \qquad (1)$$

where A_c is the area under a log-normal curve, y_o is the baseline offset, x_c is the peak center of the log-normal contribution, σ is the standard deviation of the log-normal contribution, A_r is the area under a Gaussian curve, σ_1 is the width of a Gaussian curve (= FWHM/$\sqrt{}$ln4) and x_{cg} is the peak centre of a Gaussian curve.

Results and Discussion

Four different Ge:Si precursor solutions (Ge:Si 1:4, Ge:Si 1:3, Ge:Si 1:2 and Ge:Si 1:1), at four different reaction temperatures (573, 673, 723 and 773 K) were used to grow Ge nanowires via the SCF self-seeded approach. The corresponding diameter distributions for each sample were fitted using the combined log-normal/Gaussian function shown in equation 1. Table 1 below provides a summary of the log-normal peak center, x_c, and the Gaussian peak center, x_{cg}, fits, as determined by equation 1, for each of the Ge nanowire samples produced. Independent of the precursor used, the log-normal peak centre

was seen to increase with increasing growth temperature. The log-normal peak center also increased as the Ge:Si ratio changed from 1:3 to 1:1. Both of these trends highlight the larger diameter nanowires achieved at high Ge concentrations and high growth temperatures, also illustrate the temperature dependence of a diffusion limited growth process.

Table 1. Table illustrating trends in log-normal peak centers, x_c, (coalescence) and Gaussian peak centers, x_{cg}, (Ostwald ripening) for synthesised Ge nanowires as a function of the Ge:Si precursor ratio and reaction temperature.

		Ge:Si 1:3	Ge:Si 1:2	Ge:Si 1:1
773 K	x_c	11.2 nm	---	17.4 nm
	x_{cg}	12.6 nm	21.8 nm	25.0 nm
723 K	x_c	7.6 nm	16.3 nm	21.4 nm
	x_{cg}	---	22.9 nm	---
673 K	x_c	7.2 nm	11.3 nm	13.3 nm
	x_{cg}	---	17.4 nm	---
573 K	x_c	6.2 nm	10.6 nm	14.4 nm
	x_{cg}	---	16.0 nm	---

Figure 1 shows the measured diameter distributions of self-seeded Ge nanowires formed using the Ge:Si 1:3 precursor as a function of temperature. A log-normal function fitted the diameter distribution of the nanowires grown at 573 K very well ($R^2 > 0.9$), with a primary peak centered at a diameter of 6 nm. Using the same precursor, experiments at 673 and 723 K yielded distributions with slightly larger primary peaks (7 and 8 nm respectively) but still displayed a similar log-normal compliance. The small shoulder fitted on the large diameter side of the nanowire distribution (grown at 773 K) in figure 1 may be attributed to the onset of Ostwald ripening behaviour. This diameter distribution, fitted with a log-

normal function on its own, yielded an R^2 value of 0.85. Using the combined log-normal/Gaussian function in equation 1 to account for the Ostwald ripening, an R^2 of 0.95 was achieved.

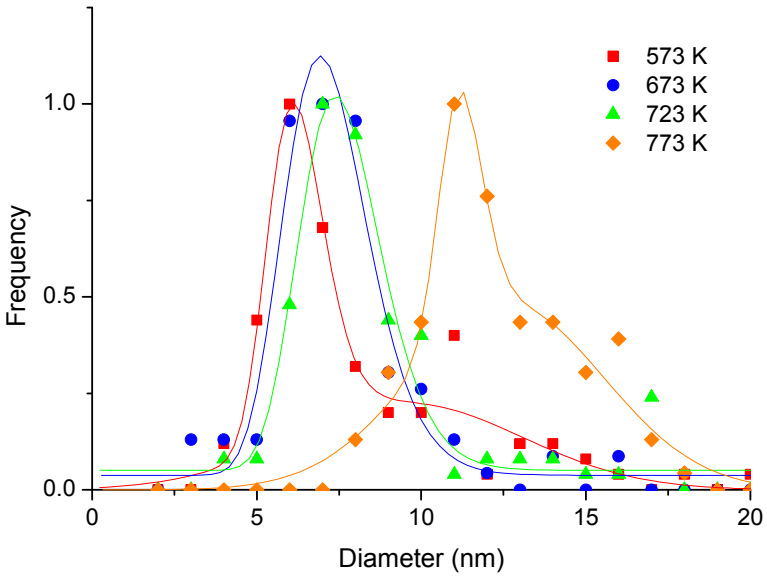

Figure 1. Diameter distributions of Ge nanowires grown from the Ge:Si 1:3 precursor at 573, 673, 723 and 773 K. A shift in the primary peak is observed as the growth temperature increased. The distributions of nanowire diameters were determined from TEM measurements of over 100 nanowires for each data set and fitted using a combined log-normal-Gaussian profile as detailed in equation 1.

Without exception, the mode seen in the diameter distributions of the Ge nanowires synthesised from the precursors increased with rising temperature and this is reflected in the log normal peak centers summarized in table 1. The driving force for any type of nucleation is an overall reduction of the Gibbs energy. A supersaturated solution will have an associated high chemical potential and the introduction of a solid phase through nucleation acts to lower this.[19] In the case of the mixed Ge:Si precursors, the supersaturation is that of local Ge supersaturation within a Si-based matrix. The first stage in the growth mechanism of these Ge nanowires is the nucleation of Ge nuclei within an amorphous $SiO_xC_yH_z$ matrix. This matrix is the shell material that surrounds some of the wires formed. Figure S1 is a combined TEM/EDX line scan image showing the amorphous nature and composition of this shell material. Following decomposition of the precursor, Ge nuclei are formed by microphase demixing followed by homogeneous nucleation of Ge from the amorphous germanium-rich $SiO_xC_yH_z$ material.

The defects in this amorphous material can act as nucleation sites with low activation energy barriers to seed the nucleation of the Ge nanoparticles. The defective regions would have high interfacial energies due to the dangling bonds present. By nucleating at such sites, the Ge atoms are able to help minimize the total interfacial free energy of the system.[20] The nuclei at this stage of growth are subject to a critical diameter depending on the precursor used and the growth temperature employed. As per nucleation theory, a critical radius exists for the nucleation of a particle. This critical radius is dependent on both concentration and temperature.[16] Nuclei below this dimension are not stable and retreat back into solution. Nuclei that satisfy this dimensional requirement are stable and are able to grow and then coalesce together within the $Si_xO_yCH_z$ matrix to form Ge particles which in turn, coalesce or fuse to form an elongated structure. Aggregation of these elongated structures will eventually form a nanowire.

Figure 2 shows a sequence of TEM images taken at 1 min intervals of some Ge:Si (1:2) precursor that was not fully decomposed from a reaction at 573 K. A large number of Ge nuclei can be observed within the Si-based matrix. Significantly, continued exposure of the Ge nanoclusters in the sample to the electron beam (200 kV) results in extra Ge nanoparticle nucleation, as shown in figures 2(a) and (b). Although the particular nucleation shown in figure 2 below is e-beam induced, it nonetheless offers an insight into the possible thermally induced nucleation that occurs from this same precursor material in the closed, pressurised reaction cell. Broadening of the particle size can be seen to occur in the latter part of the sequence; one such example is highlighted throughout the sequence by the white circles in figures 2(a) to (h). In figures 2(a) to (d), the two highlighted small particles can be seen to grow in size before coalescing together (figure 2(d)). This process is then repeated again with the now larger particle in figures 2(e) to (f).

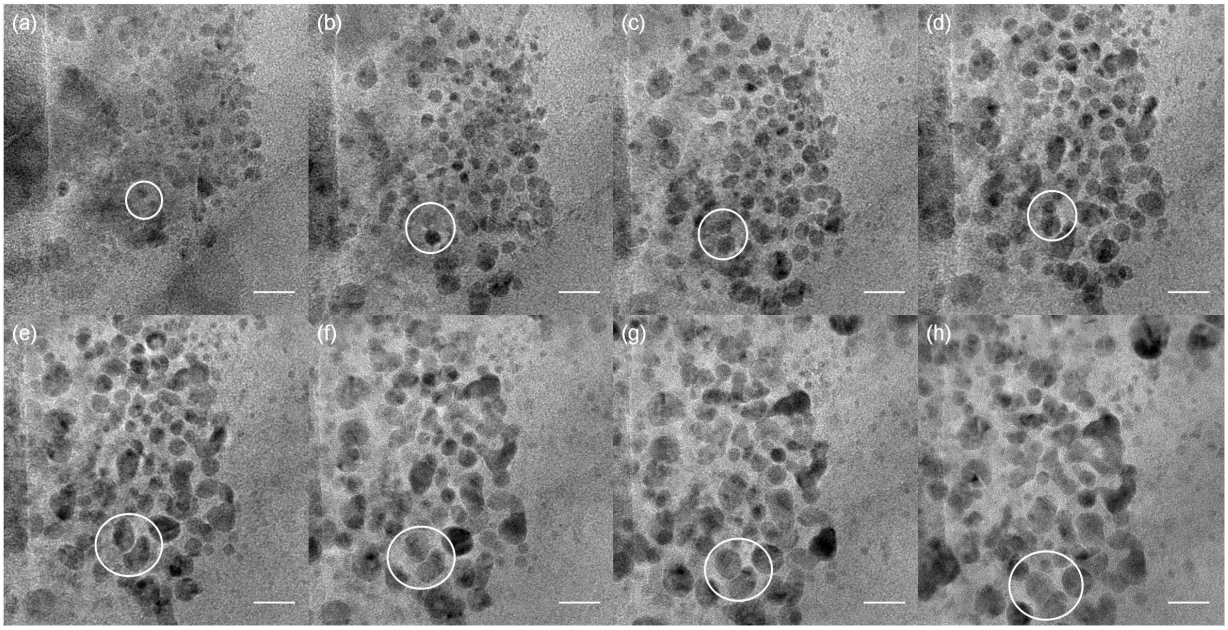

Figure 2. TEM sequence showing the nucleation, diameter broadening and coalescence of Ge nanoparticles from a Ge:Si (1:2) precursor under an electron beam (200 kV). The growth of one such particle is highlighted throughout the sequence by a white circle (scale bars = 20 nm).

The aggregation of partially formed nanowires is evidenced by a "pinch" in the nanowire diameters often imaged by TEM. We postulate that these pinches occur at the sites where the partially formed nanowires fuse together. These "pinched" sites offer further evidence that the growth mechanism of the nanowires involves the attachment of one elongated structure to another. The theory of attachment-oriented growth has been used to explain the seedless growth of PbS nanowires, also of a cubic crystal structure, by Yong *et al.*[21] They attributed the growth of the PbS nanowires to the spontaneous alignment and fusion of PbS nanoparticles to form elongated structures and tentatively suggested that the alignment is a dipole-driven oriented aggregation of nanoparticles caused by exposed high energy surface facets of the PbS crystal. However, the temporary dipoles in such structures are due to the charge balance that exists between metallic and non-metallic faces. A more likely explanation for the attachment orientated growth of Ge nanostructures is that offered by Halder *et al.*[22] in their study of gold nanowires. They propose that a smoothing process, occurring between two faceted nanoparticles, provides a symmetry breaking mechanism that allows wire growth or elongation through the formation of a neck. The neck, due to the concave nature, then creates a negative potential on the wire to which

atoms or clusters of atoms can diffuse from areas of higher potential, such as nearby flat or convex surfaces. This flux of material from areas of higher chemical potential to areas of lower chemical potential is shown schematically in figure 3 below.

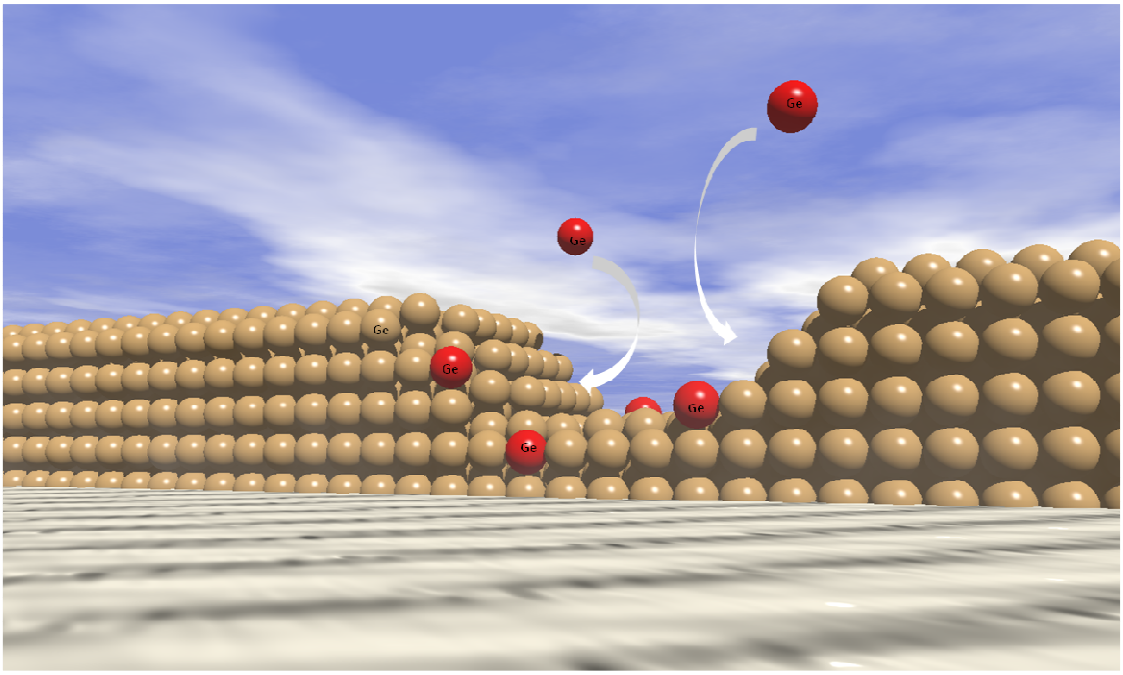

Figure 3. Schematic showing the diffusion of Ge atoms to concave sites of low chemical potential.

This smoothing process is evidenced in both the gold nanowires synthesised by Halder *et al.* and the Ge nanowires synthesised in this work by the formation of coherent twin boundaries, highlighted in figure 4(a). The twin formation is also highlighted by the FFT of the nanowire inset in figure 4(a), which clearly shows the twin relationship. This is where one set of {111} planes remain continuous while the other set of {111} planes are related by a mirror symmetry across the boundary. The coherent twin boundary, being a very low-energy interface for Ge (*ca.* ~30 mJ m^{-2}), gives rise to this possibility.[23] The pinch site is therefore eventually normalised with the rest of the nanowire diameter by Ge nuclei that continue to diffuse to the wire due to the negative radius of curvature associated with a concave notch. Once this crystalline structure is formed, Ge nuclei continue to diffuse to the formed nanowire and small Ge particles can be seen to occupy the amorphous shell material that surrounds these wires (figure 4(c)). The shell material on the nanowires is more evident at higher growth temperatures (723

and 773 K) and lower temperature growth (573 and 673 K) often exhibit wires with less shell material, and sometimes no shell material, as shown in figure 4(d). As the growth temperature is increased, there is an increase in the rate of diffusion of Ge within the $Si_xO_yCH_z$ matrix, leading to a broadening of the nanowire diameter through diffusion-limited Ostwald ripening.[24]

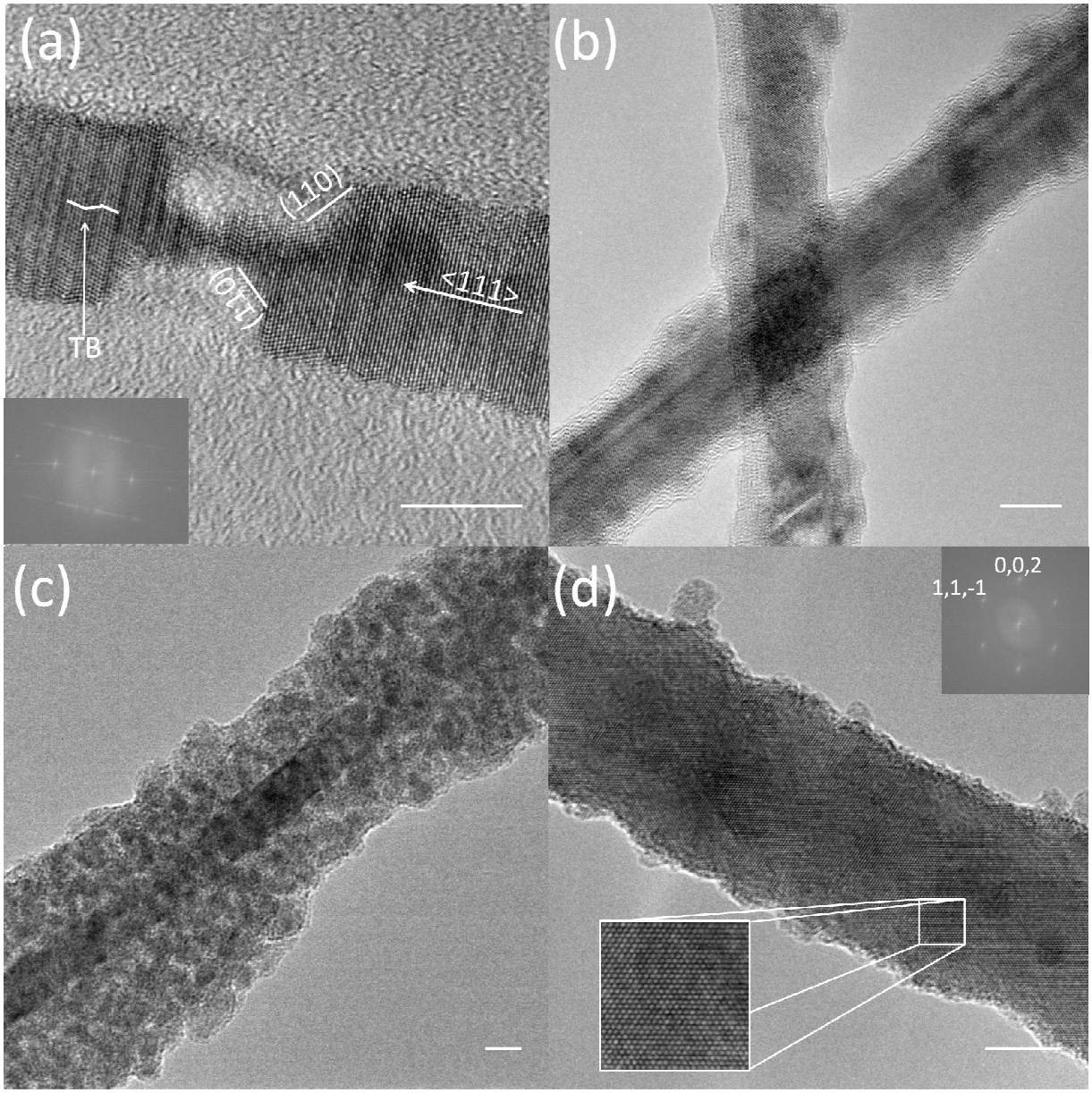

Figure 4. High resolution TEM images of (a) a "pinch" in a Ge nanowire with growth direction, high energy surface facets and twinning boundaries (TB) highlighted (insert: FFT displaying the twinning relationship), (b) Ge nanowires with amorphous shells, (c) Ge nanowire with amorphous shell containing Ge nanoparticles and (d) Ge nanowire without an amorphous shell. Insert in 3(d) shows the highly crystalline nature of the nanowires and the FFT illustrates the <111> growth direction (scale bars =10 nm).

The constant trend of increasing wire diameter with a greater Ge:Si ratio may be understood by the increased relative amount of Ge compared to silicon in the system and the dynamics of the coalescence and ripening processes of Ge in the $Si_xO_yCH_z$ matrix. Although the Ge atomic concentration in the precursors increases upon moving from Ge:Si 1:4 towards 1:1, the increase in the mode diameters observed are primarily due to the increasing Ge:Si ratio and not the total atomic concentration of Ge. To prove this hypothesis, the Ge:Si 1:3 and 1:2 precursors were matched in their atomic concentration of Ge (0.034 M) and nanowires were grown from both precursors at 573 K. The diameter distributions of both nanowire products were compared and the 1:2 precursor consistently yielded nanowires of larger mode diameter than nanowires obtained from the 1:3 precursor. An increased Ge:Si ratio therefore leads to the growth of Ge nanowires with larger mode diameters. Diffusion-limited growth of nanowires is directly related to the solute concentration in a system, which in this study is controlled by the Ge:Si ratio, where the Si forms the amorphous $Si_xO_yCH_z$ medium through which the Ge must diffuse. Fick's first law of diffusion (equation 2), states that the flux of matter between areas of high and low concentration is directly proportional to the concentration gradient that exists between these two areas of Ge content.

$$J = -D\Delta c \qquad (2)$$

where J = flux (mol m^{-2} s^{-1}) D is the diffusion coefficient (m^2 s^{-1}) and Δc is the concentration gradient. The coefficient of proportionality in this flux-concentration relationship, known as the diffusion coefficient, D, is also temperature dependant and is a function of the mean free path and mean thermal speed. As the mean thermal speed increases with temperature, the diffusivity of the nucleating clusters also increases with temperature.[25] Consequently longer, broader wires are formed at higher temperatures and at higher Ge content.

The oligosilylgermane precursors decomposed to form matrices, composing of varying compositions of C, H, Si, Ge and O, from which the Ge nanowires nucleated. As the Ge content in the Ge:Si (1:4) is comparatively small compared to Si, a reduced number of Ge nucleation events will occur compared to the other precursors investigated . The low Ge content effectively lowers the quantity of Ge atoms that can diffuse to a certain nucleus within the amorphous matrix, and no nanowire growth was observed over a reaction time of 24 h at 673 K. The observations from the Ge:Si (1:4) precursor suggests that a certain threshold concentration exists, below which insufficient nucleation occurs via diffusion. The observed threshold concentration is overcome by altering the Ge:Si ratio from 1:4 to 1:3, resulting in sufficient Ge nucleation events to generate small diameter (6 nm) Ge nanowires. As the Ge:Si ratio is increased further to 1:2 and 1:1, the mode diameter of the nanowires synthesised increase from 6 to 11 nm respectively, as is highlighted in figure 5 below. A comparison of experiments performed at 573 K show the peak centers (or mode diameters) at 6, 11 and 14 nm for the Ge:Si 1:3, Ge:Si 1:2 and Ge:Si 1:1 precursors respectively. Ostwald ripening becomes dominant when the Ge:Si ratio shifts from 1:3 towards 1:1. This increase in Ostwald ripening behaviour is reflected in the diameter distributions which are fitted with a Gaussian-like profile. At a Ge:Si ratio of 1:1, all of the Ge nanowires formed undergo so much broadening that no evidence remains of the coalescence that preceded this Ostwald ripening and so the log-normal contribution of the fitting function is effectively reduced to zero.

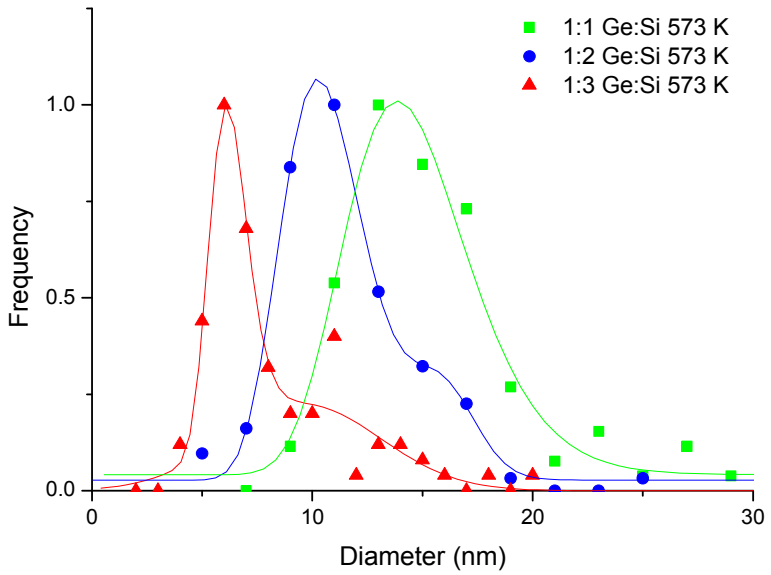

Figure 5. Fitting function of Ge nanowires formed at 573 K using the Ge:Si 1:3, Ge:Si 1:2 and Ge:Si 1:1 precursors respectively, highlighting the mode diameter shift of the nanowires generated. The distributions were determined from TEM measurements of over 100 nanowires for each sample and fitted using the combined log-normal-Gaussian function given in equation 1.

As previously discussed, Ge nanowires synthesised at a low temperature, *e.g.* 573 K and from precursors with a low Ge content, *e.g.* Ge:Si (1:3) tended to show a log-normal type diameter distribution indicative of coalescence. Experiments at a higher temperatures, *e.g.* 773 K, and from precursors with a high Ge content, e.g. Ge:Si (1:1), displayed a more Gaussian nanowire diameter distribution, indicative of Ostwald ripening. Many experiments, however, showed nanowire diameter distributions that displayed evidence of both coalescence and Ostwald ripening and were modeled sometimes using an equal contribution from both the log normal and Gaussian terms, such as the Ge:Si ratio of 1:2 at 723 K.

Conclusions

Ge nanowires have been successfully grown without the introduction of a foreign seed particle from various mixed Ge/Si precursors. A model has been proposed which accounts for nanoparticle coalescence at the beginning stage of nanowire growth and Ostwald ripening in the latter stages of

growth. Analysis of the nanowire diameter distributions revealed several trends which can be directly related to the Ge:Si ratio of the precursor employed and the growth temperature. We have shown that the information yielded from analysis of diameter distributions can aid towards the understanding of growth mechanisms in nanowire growth experiments. This study also highlights the possibility of achieving Ge nanowire diameter control through the engineering of various Ge precursor molecules.

ASSOCIATED CONTENT

Supporting Information

Combined TEM/EDX data for nanowires grown. Detail of fitting function described in equation 1. Fitted diameter distributions for all growth experiments conducted in this study. This material is available free of charge via the Internet at http://pubs.acs.org.

AUTHOR INFORMATION

Corresponding Author

*To whom correspondence should be addressed: Tel: +353 (0)21 4903608; Fax: +353 (0)21 4274097; E-mail: j.holmes@ucc.ie

Author Contributions

The manuscript was written through contributions of all authors. All authors have given approval to the final version of the manuscript.

Acknowledgements

The research leading to these results has received funding from the EU 7th Framework Programme under the SiNAPS project (Grant: 257856).

References

1. (a) Wu, X. Y.; Kulkarni, J. S.; Collins, G.; Petkov, N.; Almecija, D.; Boland, J. J.; Erts, D.; Holmes, J. D., *Chem. Mater.* **2008,** *20* (19), 5954-5967; (b) Hanrath, T.; Korgel, B. A., *J. Am. Chem. Soc.* **2004,** *126* (47), 15466-15472.

2. Chockla, A. M.; Panthani, M. G.; Holmberg, V. C.; Hessel, C. M.; Reid, D. K.; Bogart, T. D.; Harris, J. T.; Mullins, C. B.; Korgel, B. A., *J. Phys. Chem. C* **2012,** *116* (22), 11917-11923.

3. Seo, M. H.; Park, M.; Lee, K. T.; Kim, K.; Kim, J.; Cho, J., *Energy Environ. Sci.* **2011,** *4* (2), 425-428.

4. Bootsma, G. A.; Gassen, H. J., *J. Cryst. Growth* **1971,** *10* (3), 223-&.

5. Heath, J. R.; LeGoues, F. K., *Chem. Phys. Lett.* **1993,** *208* (3-4), 263-268.

6. (a) Hobbs, R. G.; Petkov, N.; Holmes, J. D., *Chem. Mater.* **2012,** *24* (11), 1975-1991; (b) Barth, S.; Hernandez-Ramirez, F.; Holmes, J. D.; Romano-Rodriguez, A., *Prog. Mater Sci.* **2010,** *55* (6), 563-627.

7. Hobbs, R. G.; Barth, S.; Petkov, N.; Zirngast, M.; Marschner, C.; Morris, M. A.; Holmes, J. D., *J. Am. Chem. Soc.* **2010,** *132* (39), 13742-13749.

8. Allen, J. E.; Hemesath, E. R.; Perea, D. E.; Lensch-Falk, J. L.; LiZ.Y; Yin, F.; Gass, M. H.; Wang, P.; Bleloch, A. L.; Palmer, R. E.; Lauhon, L. J., *Nat Nano* **2008,** *3* (3), 168-173.

9. Holmberg, V. C.; Collier, K. A.; Korgel, B. A., *Nano Letters* **2011,** *11* (9), 3803-3808.

10. Barth, S.; Koleśnik, M. M.; Donegan, K.; Krstić, V.; Holmes, J. D., *Chem. Mat.* **2011,** *23* (14), 3335-3340.

11. Granqvist, C. G.; Buhrman, R. A., *J. Catal.* **1976,** *42* (3), 477-479.

12. Senkov, O. N., *Scripta Mater.* **2008,** *59* (2), 171-174.

13. Madras, G.; McCoy, B. J., *Chem. Eng. Sci.* **2002,** *57* (18), 3809-3818.

14. Fischer, J.; Baumgartner, J.; Marschner, C., *Organometallics* **2005,** *24* (6), 1263-1268.

15. (a) Lifshitz, I. M.; Slyozov, V. V., *J. Phys. Chem. Solids* **1961,** *19* (1-2), 35-50; (b) Wagner, C., *Zeitschrift Fur Elektrochemie* **1961,** *65* (7-8), 581-591.

16. Finsy, R., *Langmuir* **2004,** *20* (7), 2975-2976.

17. (a) Senkov, O. N.; Shagiev, M. R.; Senkova, S. V.; Miracle, D. B., *Acta Mater.* **2008,** *56* (15), 3723-3738; (b) Ma, Y.; Ardell, A. J., *Acta Mater.* **2007,** *55* (13), 4419-4427; (c) Ges, A. M.; Fornaro, O.; Palacio, H. A., *Mater. Sci. Eng. A-Struct. Mater. Prop. Microstruct. Process.* **2007,** *458* (1-2), 96-100.

18. Conti, M.; Meerson, B.; Peleg, A.; Sasorov, P. V., *Physical review. E, Statistical, nonlinear, and soft matter physics* **2002,** *65* (4 Pt 2A), 046117.

19. (a) Mullin, J. W., *Crystallization*. Elsevier Science: 2001; (b) Auer, S.; Frenkel, D., *Nature* **2001,** *413* (6857), 711-713.

20. Zheng, F.; Chew, H. G.; Choi, W. K.; Zhang, J. X.; Seng, H. L., *J. Appl. Phys.* **2007,** *101* (11).

21. Yong, K. T.; Sahoo, Y.; Choudhury, K. R.; Swihart, M. T.; Minter, J. R.; Prasad, P. N., *Chem. Mater.* **2006,** *18* (25), 5965-5972.

22. Halder, A.; Ravishankar, N., *Adv. Mater.* **2007,** *19* (14), 1854-+.

23. Davidson, F. M.; Lee, D. C.; Fanfair, D. D.; Korgel, B. A., *J. Phys. Chem. C* **2007,** *111* (7), 2929-2935.

24. Chew, H. G.; Choi, W. K.; Foo, Y. L.; Zheng, F.; Chim, W. K.; Voon, Z. J.; Seow, K. C.; Fitzgerald, E. A.; Lai, D. M. Y., *Nanotechnology* **2006,** *17* (8), 1964-1968.

25. Atkins, P. W., *Physical Chemistry*. 4 ed.; Freeman: 1990.